

The bHLH Transcription Factor HBI1 Mediates the Trade-Off between Growth and Pathogen-Associated Molecular Pattern–Triggered Immunity in *Arabidopsis*^{W|OPEN}

Min Fan,^{a,1} Ming-Yi Bai,^{a,b,1} Jung-Gun Kim,^c Tina Wang,^{a,d} Eunkyoo Oh,^a Lawrence Chen,^{a,d} Chan Ho Park,^a Seung-Hyun Son,^e Seong-Ki Kim,^e Mary Beth Mudgett,^c and Zhi-Yong Wang^{a,2}

^aDepartment of Plant Biology, Carnegie Institution for Science, Stanford, CA 94305

^bThe Key Laboratory of Plant Cell Engineering and Germplasm Innovation, Ministry of Education, School of Life Sciences, Shandong University, Jinan 250100, China

^cDepartment of Biology, Stanford University, Stanford, CA 94305

^dHenry M. Gunn High School, Palo Alto, CA 94306

^eDepartment of Life Science, Chung-Ang University, Seoul 156 756, Korea

The trade-off between growth and immunity is crucial for survival in plants. However, the mechanism underlying growth-immunity balance has remained elusive. The PRE-IBH1-HBI1 tripartite helix-loop-helix/basic helix-loop-helix module is part of a central transcription network that mediates growth regulation by several hormonal and environmental signals. Here, genome-wide analyses of HBI1 target genes show that HBI1 regulates both overlapping and unique targets compared with other DNA binding components of the network in *Arabidopsis thaliana*, supporting a role in specifying network outputs and fine-tuning feedback regulation. Furthermore, HBI1 negatively regulates a subset of genes involved in immunity, and pathogen-associated molecular pattern (PAMP) signals repress *HBI1* transcription. Constitutive overexpression and loss-of-function experiments show that HBI1 inhibits PAMP-induced growth arrest, defense gene expression, reactive oxygen species production, and resistance to pathogen. These results show that HBI1, as a component of the central growth regulation circuit, functions as a major node of crosstalk that mediates a trade-off between growth and immunity in plants.

INTRODUCTION

The trade-off between growth and immunity is crucial for optimal survival of plants in nature and is also important for agricultural productivity of crops. This trade-off is believed to require complex interactions between signal transduction pathways activated by growth signals and pathogen-generated signals (Robert-Seilaniantz et al., 2011). Plant growth is regulated by a wide range of signals, including endogenous hormones and environmental cues, such as light, temperature, and the presence of pathogens. These hormonal and environmental signals act through distinct signal transduction pathways, which have been studied extensively. Interactions between these pathways have also been observed at the molecular level (Depuydt and Hardtke, 2011), but the key molecular junctions regulated by both hormone and defense signaling pathways has remained elusive.

Brassinosteroids (BRs) are a group of growth-promoting hormones that regulate many developmental responses and also modulate immunity. BRs act through a well-defined signal

transduction pathway (Kim and Wang, 2010; Wang et al., 2012). BRs directly interact with the extracellular domains of the receptor kinases BRASSINOSTEROID-INSENSITIVE1 (BRI1) and SOMATIC EMBRYOGENESIS RECEPTOR KINASE1 to induce their dimerization and *trans*-phosphorylation (Li et al., 2002; Nam and Li, 2002; Wang et al., 2008; Santiago et al., 2013). Activated BRI1 phosphorylates downstream receptor-like cytoplasmic kinase proteins BR-SIGNALING KINASE (BSK) and CONSTITUTIVE DIFFERENTIAL GROWTH1, which in turn phosphorylate and activate members of the BRI1 SUPPRESSOR1 (BSU1) family of phosphatases (Tang et al., 2008; Kim et al., 2009, 2011). BSU1 inactivates the GSK3-like kinase BRASSINOSTEROID-INSENSITIVE2 (BIN2) through Tyr dephosphorylation (Kim et al., 2009), leading to activation of BIN2's substrates BRASSINAZOLE-RESISTANT1 (BZR1) and BZR2 (also named BRI1-EMS-SUPPRESSOR1 [BES1]) by PP2A-mediated dephosphorylation (Tang et al., 2011). Dephosphorylated BZR1 and BZR2 translocate into the nucleus to regulate the expression of BR response genes (Sun et al., 2010; Yu et al., 2011).

The transcriptional activity of BZR1 depends on its interactions with proteins regulated by other signaling pathways, including the PHYTOCHROME-INTERACTING FACTORS (PIFs) regulated by light, temperature, and circadian clock, and the DELLA proteins regulated by gibberellin (GA) (Bai et al., 2012b; Oh et al., 2012). BZR1 interacts with PIFs, which accumulate when plants are in the dark or shade, at promoters of common target genes to activate gene expression and promote cell elongation (Oh et al., 2012). The DELLA proteins, which accumulate when GA levels are low (Sun, 2011),

¹ These authors contributed equally to this work.

² Address correspondence to zywang24@stanford.edu.

The author responsible for distribution of materials integral to the findings presented in this article in accordance with the policy described in the Instructions for Authors (www.plantcell.org) is: Zhi-Yong Wang (zywang24@stanford.edu).

^{W|OPEN} Online version contains Web-only data.

^{OPEN} Articles can be viewed online without a subscription.

www.plantcell.org/cgi/doi/10.1105/tpc.113.121111

inhibit the DNA binding activities of both BZR1 and PIFs (de Lucas et al., 2008; Feng et al., 2008; Bai et al., 2012b; Gallego-Bartolomé et al., 2012; Li et al., 2012). Therefore, the direct interactions among BZR1, PIF4, and DELLA integrate BR, phytochrome, and GA signals to regulate plant growth (Bai et al., 2012b; Oh et al., 2012; Wang et al., 2012).

The promotion of cell elongation by the BZR1-PIF4 module requires the PRE-IBH1-HBI1 tripartite helix-loop-helix/basic helix-loop-helix (HLH/bHLH) module. BZR1-PIF4 transcriptionally activates members of the PACLOBUTRAZOL-RESISTANT (PRE) family of non-DNA binding HLH factors, which sequester several HLH factors that otherwise inhibit DNA binding bHLH factors (Bai et al., 2012a; Oh et al., 2012). For example, PRE1 and PRE6/KIDARI interact with HFR1 and PAR1, which both inhibit PIF4 DNA binding, forming positive feedback loops (Hyun and Lee, 2006; Hornitschek et al., 2009; Hao et al., 2012). PRE1 also binds to IBH1 to prevent its inhibition of the bHLH factors HBI1 and ACTIVATORS FOR CELL ELONGATION (ACE1 to ACE3) (Bai et al., 2012a; Ikeda et al., 2012). Together, the BZR-PIF4 and HLH/bHLH modules form a central growth regulation transcription network that integrates hormonal and environmental signals. While genetic evidence supports an important role for HBI1 in promoting cell elongation (Bai et al., 2012a), the molecular functions of HBI1 in integrating signals into the network and specifying output remain unclear.

Pathogen-associated molecular pattern (PAMP) signals and growth-promoting hormones are known to antagonize each other to mediate the trade-off between growth and immunity, which is important for plant survival (Robert-Seilaniantz et al., 2011). The growth-promoting hormones BR and auxin inhibit PAMP-triggered immunity (PTI), and PAMPs (e.g., flagellin and elongation factor peptides flg22 and elf18, respectively) inhibit plant growth. Interactions between the BR and flagellin pathways have been studied extensively (Chinchilla et al., 2007; Kemmerling et al., 2007; Albrecht et al., 2012; Belkhadir et al., 2012; Lin et al., 2013; Shi et al., 2013). The BR receptor kinase BRI1 and the flagellin receptor kinase FLS2 share the coreceptor BAK1 and the substrates BSK1 and BOTRYTIS-INDUCED KINASE1 (BIK1) (Chinchilla et al., 2007; Kemmerling et al., 2007; Lin et al., 2013; Shi et al., 2013). BIK1 can be phosphorylated by both FLS2-BAK1 and BRI1, and positively regulates flagellin signaling but negatively regulates BR signaling (Lu et al., 2010; Lin et al., 2013). The functional importance of these shared components in the communication between the two pathways remains controversial. While BRI1 was shown to modulate FLS2 signaling through both BAK1-dependent and BAK1-independent mechanisms, BR does not affect the formation of the flg22-triggered FLS2-BAK1 complex (Albrecht et al., 2012; Belkhadir et al., 2012; Lozano-Duran et al., 2013). Furthermore, the weak effects of BR on flg22-induced BIK1 phosphorylation suggested that major crosstalk between the BR and FLS2 pathways occurs downstream of the membrane-bound kinases (Albrecht et al., 2012). A recent study reported that the activated BZR1 associates with WRKY40 to mediate repression of immune responses (Lozano-Duran et al., 2013). However, BES1/BZR2 was shown to be unaffected by PAMP signals (Albrecht et al., 2012), although whether BZR1 is affected by PAMPs remains unclear. Therefore, the major junction regulated by both PAMP and BR pathways might be downstream of BZR1.

Here, we performed chromatin immunoprecipitation followed by sequencing (ChIP-Seq) and RNA sequencing (RNA-Seq) experiments to identify the target genes of HBI1 in the *Arabidopsis thaliana* genome. The results show that HBI1 has overlapping functions with PIFs in activating genes involved in cell elongation but distinct functions in feedback regulation of the HLH/bHLH network and in regulating chloroplast function and immune responses. The expression of *HBI1* and several homologs is repressed by PAMP signals, constitutive overexpression of *HBI1* reduces PAMP-induced immune responses, and knock-down of *HBI1* expression increases the resistance to bacterial infection. This study demonstrates that HBI1, as a key node of the central growth regulation network, mediates the integration of hormonal, environmental, and pathogen signals and plays a key role in the trade-off between immunity and growth.

RESULTS

Genome-Wide Identification of HBI1 Binding and Regulated Genes

To understand the functions of HBI1, we mapped HBI1's genomic binding sites using ChIP-Seq. Transgenic *Arabidopsis* plants expressing the HBI1 and yellow fluorescent protein (YFP) fusion protein driven by the native *HBI1* promoter were used to carry out ChIP-Seq experiments with an anti-YFP antibody. A *35S:YFP* transgenic line was used as a negative control. Analysis of the ChIP-Seq data with the statistical software CisGenome and PRI-CAT identified 1477 and 1851 HBI1 binding peaks, respectively. Among them, 1103 peaks were identified by both statistical methods and thus considered high-confidence HBI1 binding peaks and used for further analysis. The 1103 HBI1 binding peaks were linked to 1447 neighbor genes that were considered high-confidence HBI1 target genes (Figure 1A; Supplemental Data Set 1). The HBI1 target genes are distributed throughout the genome but are rare in the centromere regions (Figure 1A). Most of the HBI1 binding peaks are in the promoter regions (Figure 1B), consistent with HBI1's molecular function as a transcription factor. A motif analysis showed that CACATG, the hormone up at dawn element (Michael et al., 2008), was the most enriched *cis*-element in the HBI1 binding sites, and the G-box motif (CACGTG) was also enriched but to a lesser degree (Figure 1C).

To further define the HBI1-regulated genes, we performed RNA-Seq analysis of the transcriptomes of wild-type and transgenic *Arabidopsis* plants overexpressing *HBI1* (*HBI1-Ox*). Plants were grown on half-strength Murashige and Skoog (MS) medium with 1% Suc under constant light for 5 d. RNA-Seq analysis identified 1257 genes that were affected >1.5-fold in *HBI1-Ox* compared with the wild type (Figure 1D; Supplemental Data Set 2). Quantitative RT-PCR analyses of 14 genes confirmed the gene expression changes identified by RNA-Seq (Supplemental Table 1). Among the HBI1-regulated genes, 156 out of 600 (26%) HBI1-induced genes and 21 out of 657 (3.2%) HBI1-repressed genes are HBI1 binding targets identified in the ChIP-Seq experiment, suggesting that HBI1 is a transcription activator for most of its target genes. These 177 HBI1-regulated genes were considered functional targets of HBI1 (Figure 1D;

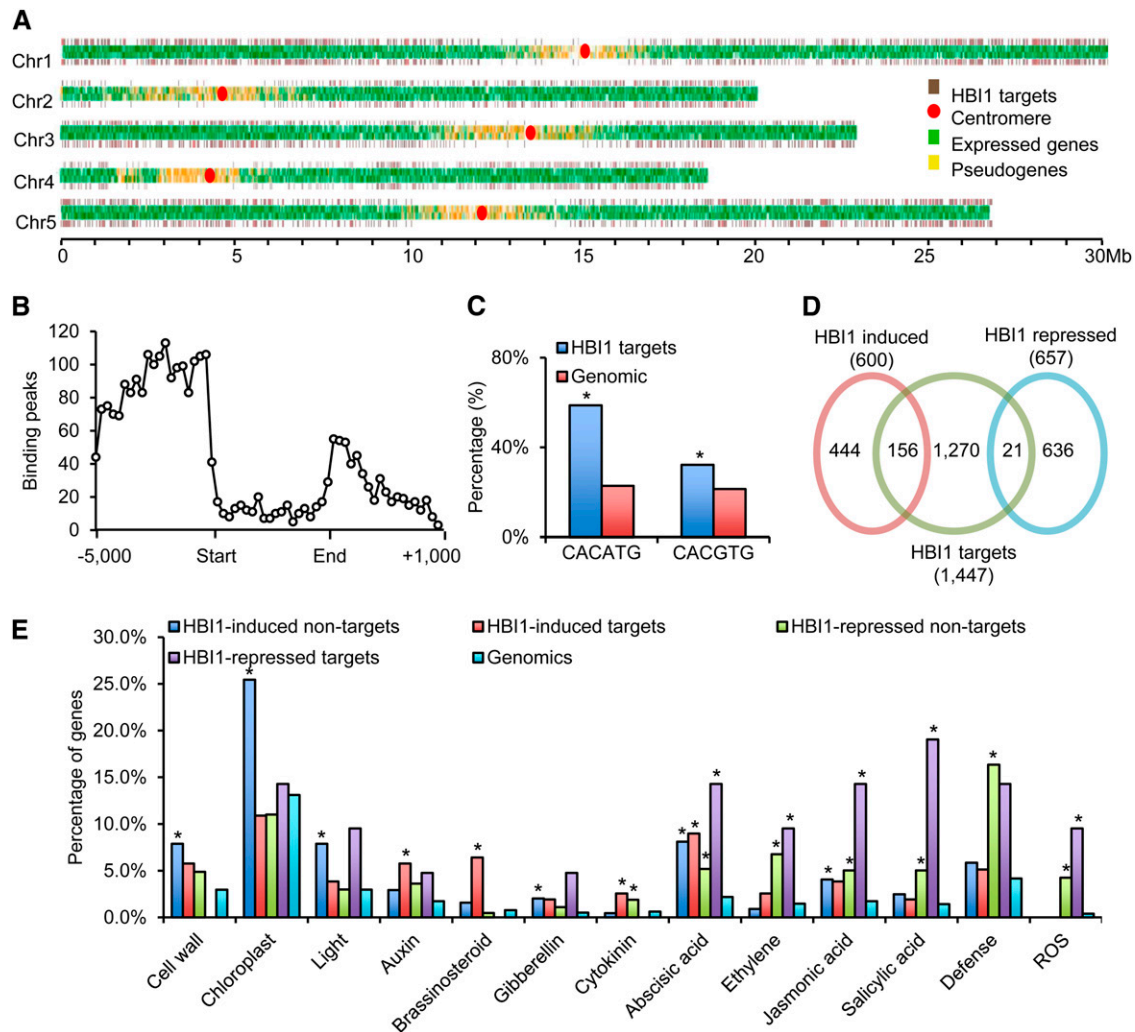


Figure 1. Genome-wide Identification of HBI1 Binding and Regulated Genes.

(A) Distribution of HBI1 binding sites along the five chromosomes of *Arabidopsis*. The HBI1 target genes are depicted by brown bars, normal expressed genes are depicted by green bars, and pseudogenes are depicted by yellow bars. A red circle indicates the location of the centromere.

(B) Distribution of HBI1 binding peaks (frequency) relative to gene structure (−5 kb to +1 kb downstream of 3' end).

(C) Frequency of shown *cis*-elements around HBI1 binding regions. Asterisk indicates significant difference from random genome (Fisher's exact test; * $P < 0.05$).

(D) Venn diagram showing the overlap between the HBI1-regulated genes and HBI1 direct target genes.

(E) Gene Ontology analyses of HBI1 directly and indirectly regulated genes. Numbers indicate the percentages of genes belonging to each Gene Ontology category. Asterisk indicates significant difference from random genome (Fisher's exact test; * $P < 0.05$).

Supplemental Data Set 2). The overlap between HBI1-affected genes and the HBI1 binding target genes seems small and may be due to different tissues used in the experiments; however, similar levels of overlap has been reported for other transcription factors (Yu et al., 2011).

Functional classification of the HBI1 binding (i.e., target) and/or HBI1-regulated (i.e., induced or repressed) genes based on Gene Ontology categories showed that HBI1 directly and indirectly regulates a range of biological processes and cellular activities (Figure 1E; Supplemental Figure 1). For example, the genes involved in cell growth and chloroplast function were highly enriched

in HBI1-induced, non-HBI1 targets. The genes involved in light response were enriched in HBI1-induced, HBI1 target, and non-target genes. The genes involved in response to growth-promoting hormones such as BR and GA were enriched in HBI1-activated HBI1 target genes. By contrast, the genes involved in responses to stress hormones, including ethylene, jasmonic acid, and salicylic acid, were enriched in HBI1-repressed HBI1 target genes. The genes involved in auxin and abscisic acid response were enriched in both HBI1-activated and HBI1-repressed genes. In addition, the genes involved in defense and reactive oxygen species (ROS) production were highly enriched in HBI1-repressed, HBI1 targets,

and nontarget genes, suggesting that HBI1 plays a role in repressing the plant defense response (Figure 1E; Supplemental Figure 1).

HBI1 activates, mostly directly, the growth-inhibiting HLH factors, such as IBH1, AIF1, AIF2, AIF3, AIF4, UPB1, PAR1, PAR2, HFR1, and three additional IBH1 homologs (At4G30180, At5G57780, and At4G30410) (Supplemental Figures 1, 2A, and 2B and Supplemental Data Set 2). A number of DNA binding bHLH factors are repressed by *HBI1-Ox*. Such extensive upregulation of the inhibitory HLH factors, many of which bind to and inactivate HBI1 and/or PIFs, suggests that a general feedback mechanism is built into the HLH/bHLH network to provide buffering function to the system.

Several gene families, many involved in defense and redox regulation, are consistently repressed by *HBI1* overexpression (Supplemental Figure 1). These include about 31 cytochrome P450 genes, seven WRKY transcription factors, four VQ motif-containing proteins, three U-box proteins, four calmodulin-like proteins, nine FAD binding Berberine family proteins, 11 glutathione *S*-transferases, and nine members of the 2-oxoglutarate and Fe(II)-dependent oxygenase superfamily (Supplemental Figure 1). In addition, HBI1 activates four (*GASA3*, 4, 6, and 7) and represses one (*GASA5*) of the 14 members of the *GASA* gene family (Roxrud et al., 2007), three of them are direct target genes of HBI1 (Supplemental Figure 1 and Supplemental Data Set 2). The *GASA* genes encode secreted Cys-rich proteins that have been implicated in development, stress response, and inhibiting ROS (Ko et al., 2007; Rubinovitch and Weiss, 2010; Nahirniak et al., 2012; Sun et al., 2013).

A previous study showed that HBI1 is a positive regulator of BR responses (Bai et al., 2012a). The ChIP-Seq results showed that many genes encoding BR biosynthetic and signaling components are HBI1 targets (Figure 2A). Quantitative ChIP-PCR and RT-PCR confirmed that HBI1 directly activates the expression of the BR biosynthetic genes *CPD*, *DWF4*, and *BR6OX1* (Figures 2B and 2C), suggesting HBI1 positively regulates BR biosynthesis. Consistent with the positive effects of *HBI1-Ox* on BR biosynthesis and signaling, the transgenic plants overexpressing *HBI1* showed increased BZR1 accumulation and dephosphorylation (Figure 2D).

HBI1 and PIF Have Overlapping and Distinct Functions

Previous studies showed that HBI1 and PIFs promote cell elongation and bind to E-box and G-box elements (Bai et al., 2012a; Oh et al., 2012). To understand the relationship between these transcription factors, we compared the genomic targets of HBI1 to those of PIF1, PIF3, PIF4, or PIF5 (Oh et al., 2009, 2012; Hornitschek et al., 2012; Zhang et al., 2013). Of the 1477 HBI1 target genes, 1054 (71.4%) were also targets of at least one of the four PIFs (Figure 3A). A comparison between the HBI1-regulated genes and the PIF-regulated genes identified based on differential expression in the *pifq* mutant (*pif1 pif3 pif4 pif5*) (Oh et al., 2012) showed that HBI1 and PIFs coregulate 720 genes, which include 464 genes (64.4%) regulated in the same direction and 256 (35.6%) in opposite direction (Figure 3B).

The genes activated by both HBI1 and PIFs include a high percentage of direct targets of HBI1 (30.7%) and PIFs (53.8%), whereas genes repressed by both HBI1 and PIFs showed the

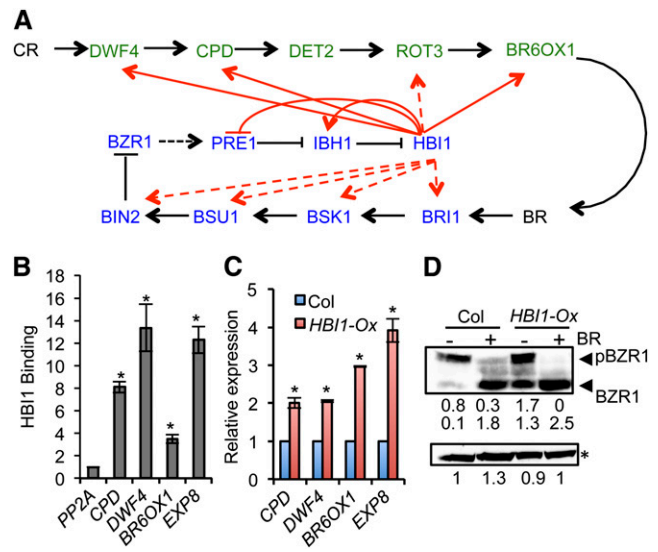


Figure 2. HBI1 Positively Regulates Components of the BR Pathway.

(A) A diagram of BR pathway. The BR biosynthetic enzymes are shown in green, and the BR signaling components are in blue. Black arrows and bar ends show activation and inhibition at the protein level. Red arrows show HBI1 binding to the promoter of these genes, with solid lines indicating HBI1 activation and dashed lines indicating no evidence for HBI1 regulation according to our RNA-Seq data.

(B) Quantitative ChIP-PCR analysis of HBI1 binding to the promoter of selected genes. The chromatin of *pHBI1::HBI1-YFP* and *35S::YFP* transgenic plants was immunoprecipitated with anti-YFP antibody, and the precipitated DNA was quantified by quantitative PCR. Enrichment of DNA was calculated as the ratio between *pHBI1::HBI1-YFP* and *35S::YFP*, normalized to that of the *PP2A* coding region. Error bars indicate standard deviation of three biological repeats. Asterisk indicates significant difference from control gene *PP2A* (*t* test; **P* < 0.05).

(C) qRT-PCR analysis of the expression of BR biosynthetic genes in the wild-type (Columbia [Col]) and *HBI1-Ox*. Error bars indicate standard deviation of three biological repeats. Asterisk indicates significant difference from wild-type control (*t* test; **P* < 0.05).

(D) Anti-BZR1 immunoblot analysis of BZR1 phosphorylation status in 4-week-old plants. The relative band intensity was quantified by ImageJ software and labeled under the gel. Asterisk indicates the non-specific bands to show equal loading. Experiment was repeated four times with similar results.

random probability of being direct targets, consistent with both HBI1 and PIFs acting mostly as transcription activators (Figure 3B). A significant portion of the genes activated by HBI1 but not affected by PIFs were also targets of HBI1 (28.4%) and PIFs (42.7%) (Figure 3B). These genes might be regulated by HBI1 and PIFs in an additive or redundant manner and thus are not affected in the *pifq* mutant.

Gene Ontology analysis showed that the genes activated by both HBI1 and PIFs are highly enriched with genes involved in BR and GA responses and cell elongation, which is consistent with HBI1's function in promoting cell elongation downstream of these hormone pathways (Supplemental Figure 3A). Chromatin immunoprecipitation-quantitative PCR (ChIP-qPCR) assays confirmed that both HBI1 and PIF4 bind to the promoters of *EXP1* and *EXP8* (Figure 3C). Quantitative RT-PCR analysis showed that

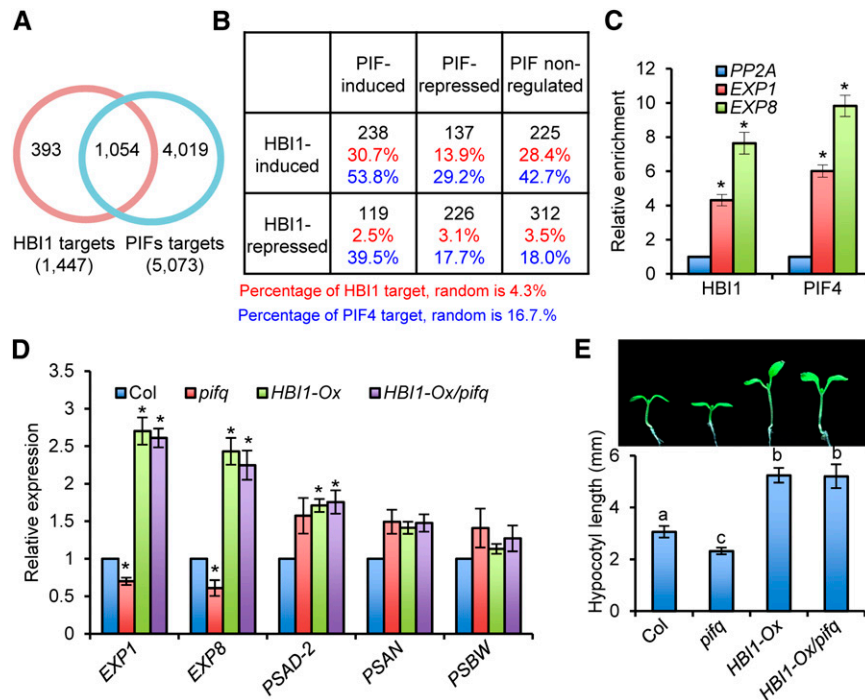


Figure 3. HBI1 and PIF Have Overlapping and Distinct Functions.

(A) Venn diagram showing the overlap between HBI1 target genes and PIF target genes. The PIF target genes include the genes associated with PIF1, PIF3, PIF4, or PIF5.

(B) The table shows the overlap of HBI1-regulated genes and PIF-regulated genes and the percentage of HBI1 target genes or PIFs target genes among the gene sets that HBI1 and/or PIFs regulate. The top black numbers are the numbers of genes regulated by HBI1 and/or PIFs, the middle red numbers are the percentage of HBI1 targets, and the bottom blue numbers are the percentage of PIF targets.

(C) ChIP-qPCR analysis of HBI1 and PIF4 binding to the promoters of selected genes. Chromatin immunoprecipitation was performed with anti-YFP antibody or anti-Myc antibody using *pHBI1:HBI1-YFP*, *35S:YFP*, *pPIF4:PIF4-myc/pifq*, and *pifq* plants grown in the dark for 5 d. Enrichment of DNA was calculated as the ratio between *pHBI1:HBI1-YFP* and *35S:YFP*, or *pPIF4:PIF4-myc/pifq* and *pifq*, normalized to that of the *PP2A* coding region as the internal control. Error bars indicate standard deviation of three biological repeats. Asterisks indicate significant difference from control gene *PP2A* (*t* test; **P* < 0.05).

(D) qRT-PCR analyses of *EXP1*, *EXP8*, *PSAD-2*, *PSAN*, and *PSBW* mRNA levels in wild-type (Col), *pifq*, and *HBI1-Ox/pifq* plants. *PP2A* was used as the internal control. Error bars indicate standard deviation from three biological repeats. Asterisks indicate significant difference from the wild type (*t* test; **P* < 0.05).

(E) Overexpression of *HBI1* rescues the dwarf phenotype of *pifq*. The top picture shows Columbia, *pifq*, *HBI1-Ox*, and *HBI1-Ox/pifq* grown for 7 d under constant light. Bottom graph shows the quantification of hypocotyl lengths. Error bars indicate standard deviation from 20 biological repeats. Different letters indicate statistically significant differences between the samples (*t* test, *P* < 0.05).

the expression levels of *EXP1* and *EXP8* were reduced in the *pifq* mutant but increased by overexpression of *HBI1* (Figure 3D). Consistent with the levels of expansin gene expression, the *pifq* mutant had shorter hypocotyls, but this defect was more than rescued by overexpression of *HBI1* (Figure 3E). Overexpression of *HBI1* also rescued additional phenotypes of the *pifq* mutant, including dwarfism and deetiolation in the dark (Supplemental Figure 3B). These results suggest that HBI1 and PIFs have interchangeable biochemical activities in regulating plant growth and photomorphogenesis.

On the other hand, the 226 genes regulated in opposite ways by HBI1 and PIFs suggest that HBI1 also has unique functions in a subset of responses (Supplemental Data Set 2). For example, the genes involved in light response and chloroplast/photosynthesis, such as *PSAD-2*, *PSAN*, and *PSBW*, are enriched in the HBI1-induced but PIF-repressed gene class (Figure 3D; Supplemental

Figure 1). Genes involved in defense, salicylic acid-dependent responses, and ethylene-dependent responses are enriched in the gene sets that are repressed by HBI1 but unaffected or affected by PIFs in complex ways (Supplemental Figure 3A).

HBI1 Is a Negative Regulator for Flagellin-Regulated Gene Expression

The HBI1 inhibition of genes involved in defense responses prompted us to further analyze the relationship between HBI1 and immunity pathways. A comparison of the *HBI1-Ox* RNA-Seq data with the previously identified microarray data sets of genes affected by *flg22* (Denoux et al., 2008) showed that 440 (35%) of the HBI1-regulated genes were affected by *flg22*, of which 355 genes (80.7%) were regulated by HBI1 and *flg22* in opposite directions, with a correlation coefficient $R = -0.47$ (Figures 4A

and 4B). Similar negative correlation was found between HBI1-mediated gene expression changes and those caused by another PAMP signal, elf18 (Tintor et al., 2013) (Supplemental Figures 4A and 4B). These data suggest that HBI1 negatively regulates a subset of PAMP-induced defense genes.

Gene Ontology analyses showed that the subset of HBI1-activated but flg22-repressed genes is enriched with cell wall- and chloroplast-related functions (Figure 4C). These data suggest that flg22 may repress cell elongation and photosynthetic functions partly through an HBI1-dependent mechanism. Strikingly, many of the defense-related genes activated by flg22 are repressed by HBI1 (Figure 4C; Supplemental Figure 1). These include many WRKY transcription factors and their interacting partner VQ-motif proteins, the plant U-box proteins, calmodulin-like proteins, and NBS-LRR proteins (Supplemental Figure 1). In addition, genes involved in ROS metabolism were dramatically enriched in the HBI1-repressed but flg22-induced genes (Figure 4C; Supplemental Figure 1). On the other hand, three of the four HBI1-induced GASA genes were repressed by flg22 (Supplemental Figure 1). These observations suggest that HBI1 is a negative regulator of PAMP-induced responses.

To confirm the RNA-Seq data, we performed quantitative RT-PCR (qRT-PCR) on selected genes. Among the HBI1-regulated target genes (Supplemental Data Sets 1 and 2), *SIB1* and *GASA4* have been recently reported to play important roles in immunity. Both loss- and gain-of-function genetic analysis demonstrated that *SIB1* is a positive regulator for the expression of several defense genes and resistance to bacterial pathogen *Pseudomonas syringae* pv *tomato* DC3000 (*Pst* DC3000) and necrotrophic fungal pathogen *Botrytis cinerea* (Xie et al., 2010; Lai et al., 2011). ChIP-qPCR analysis showed that HBI1 binds to the *SIB1* promoter (Figure 4D), and qRT-PCR analysis showed that the flg22-induced *SIB1* expression was dramatically repressed in the *HBI1-Ox* plants (Figure 4E). By contrast, the expression level of *GASA4*, which represses ROS production (Rubinovich and Weiss, 2010), is repressed by flg22 but directly activated by HBI1 (Figures 4D and 4F). The flg22 induction of *SIB1* is diminished and repression of *GASA4* is abolished in the *HBI1-Ox* plants (Figures 4E and 4F). qRT-PCR analyses of additional pathogen response genes showed that the expression levels of *FRK1*, *At2g17740*, *PR1*, *JAZ6*, and *MPK11* were increased by flg22 application in wild-type plants, but their induction was significantly reduced in the *HBI1-Ox* plants, and the expression levels of *FRK1*, *At2g17740*, *PR1*, and *MPK11* were also much lower in *HBI1-Ox* plants compared with the wild type without flg22 treatment (Figure 4G; Supplemental Figures 5A to 5D). Flg22 activation of *MPK3/6* seemed normal or slightly enhanced in the *HBI1-Ox* plants (Supplemental Figure 5E), suggesting that reduced *MPK11* expression has no effect on PAMP activation of other mitogen-activated protein kinases, consistent with that observed in the *mpk11* mutant (Bethke et al., 2012). These results demonstrate that flg22 repression of *HBI1* mediates the regulation of a subset of defense response genes.

The opposite effects of HBI1 and PAMP signals on gene expression suggest that PAMPs may inhibit HBI1 activity and/or HBI1 may repress a branch of PAMP-elicited signaling pathways. Based on microarray data (Denoux et al., 2008; Tintor et al., 2013), both flg22 and elf18 inhibit the expression of *HBI1*.

Our qRT-PCR assays verified that flg22 treatment decreases the transcript levels of *HBI1* and some of its homologs (i.e., *BEE1*, *BEE2*, *BEE3*, and *CIB1*) (Figure 4H; Supplemental Figure 6). The level of HBI1-YFP protein expressed from the endogenous *HBI1* promoter decreased rapidly after flg22 treatment, whereas the HBI1-YFP protein expressed from the constitutive 35S promoter did not change dramatically upon flg22 treatment (Figure 4I), indicating that flg22 mainly regulates HBI1 at the transcriptional level. Flg22 repression of *HBI1* expression and the inhibitory effects of *HBI1* overexpression on many flg22-induced genes indicate that HBI1 mediates flagellin regulation of a subset of genes.

HBI1 Negatively Regulates PAMP Responses

Next, we tested if the repression of *HBI1* expression contributes to the flg22-triggered growth inhibition and immunity responses. Indeed, the growth of *HBI1-Ox* was much less inhibited by flg22 and elf18 than that of wild-type plants (Figure 5A; Supplemental Figures 4D and 4E), indicating that normal PAMP inhibition of plant growth requires repression of *HBI1* expression.

The effects of *HBI1* overexpression on PAMP-induced defense gene expression suggested that HBI1 might also modulate immunity. As part of the defense mechanism, ROS production is induced by flg22 or elf18 treatment in wild-type plants, but the ROS response was slower and reached a lower magnitude in the *HBI1-Ox* plants (Figure 5B; Supplemental Figure 4F). By contrast, the flg22-elicited ROS response occurred earlier in the *HBI1* co-suppressing plants (*HBI1-CS*) compared with the wild type (Figure 5B), confirming a role of HBI1 in inhibiting ROS production.

We next tested the susceptibility of plants to infection with the virulent hemibiotrophic bacterium *Pst* DC3000. Without flg22 treatment, the *HBI1-Ox* plants exhibited a similar level of susceptibility as wild-type plants. Pretreatment of wild-type plants with flg22 markedly reduced bacterial growth due to activation of PTI (Figure 5C), but this effect of flg22 on bacterial growth was significantly reduced in the *HBI1-Ox* plants (Figure 5C), indicating that repression of *HBI1* expression is required for flagellin to fully induce immunity. Furthermore, the *HBI1-CS* plants were more resistant to *Pst* DC3000 than the wild type without flg22 pretreatment, demonstrating that HBI1 is an essential negative regulator of immunity and that reducing *HBI1* expression is sufficient to partly turn on immune responses. Interestingly, the *HBI1-CS* plants were less resistant to *Pst* DC3000 than wild-type plants after flg22 pretreatment. One possibility is that the *HBI1-CS* plants, due to the feedback regulation of HLH factors by HBI1, have an elevated level/activity of homologous bHLH factors that are not repressed by flg22. Alternatively, HBI1 might be involved in other feedback desensitization mechanisms, and long-term reduction of HBI1 level leads to decreased flg22 elicitation of immunity. In contrast with HBI1, the dominant active *bzr1-1D* and cyan fluorescent protein (CFP) fusion protein expressed from the native *BZR1* promoter had little effect on the susceptibility to *Pst* DC3000.

The *Pst* DC3000 Δ *hrcU* mutant is defective in effector delivery and lacks the effector-mediated dampening of host PTI and thus shows reduced growth in wild-type leaves compared with *Pst* DC3000 (Figure 5D). *Pst* DC3000 Δ *hrcU* grew to higher titers in the *HBI1-Ox* plants than in wild-type plants (Figure 5D),

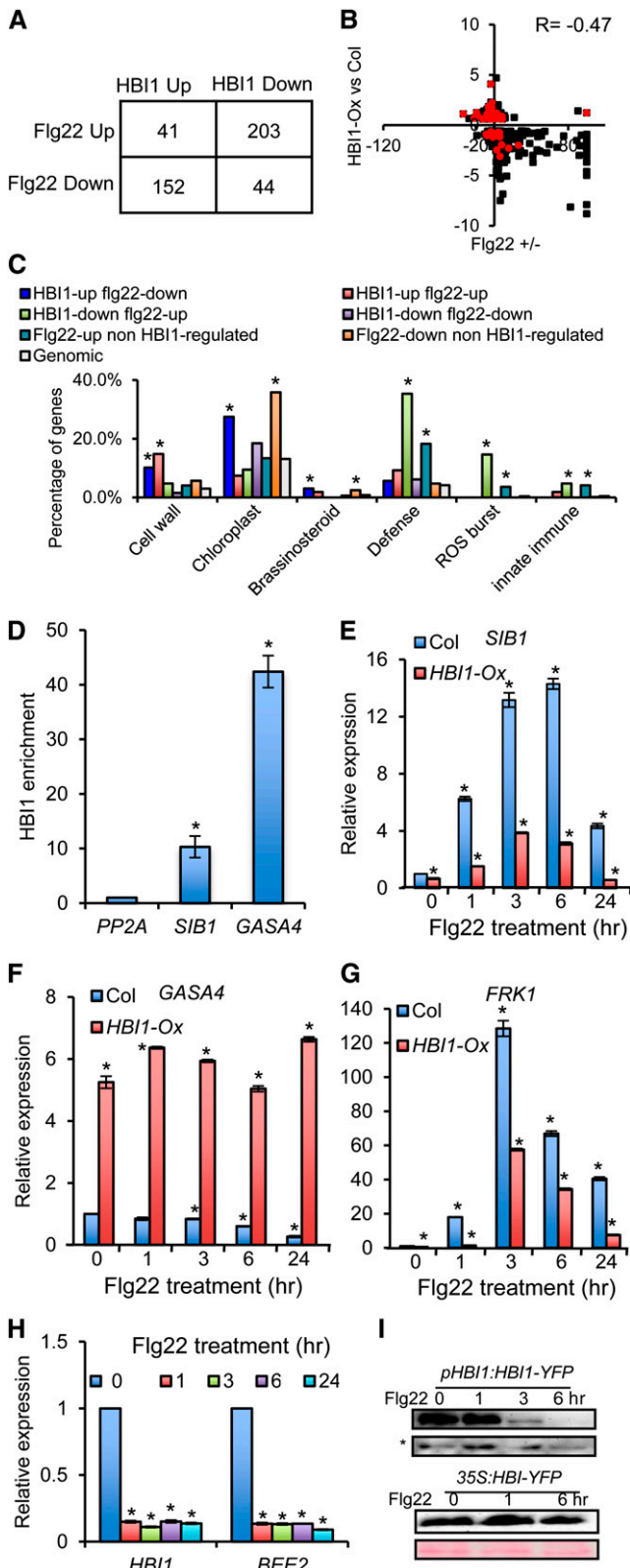


Figure 4. HBI1 and Flg22 Oppositely Regulate Gene Expression. **(A)** Overlaps between gene sets regulated by HBI1 and flg22.

consistent with the observation that HBI1 suppresses flg22-induced resistance (Figure 5C). *Pst* DC3000 $\Delta hrcU$ grew normally in the *HBI1-CS* plants compared with its growth in wild-type and *bzr1-1D-CFP* plants (Figure 5D). This is also consistent with the weak response of *HBI1-CS* plants to flg22 elicitation (Figure 5C). One possibility suggested by this observation is that the wild-type *HBI1* gene is not functional in regulating immunity against *Pst* DC3000 $\Delta hrcU$ because *HBI1* is fully inactivated by PAMP signaling triggered by this nonpathogenic strain. Taken together, these results demonstrate that the growth regulator HBI1 is a negative regulator of immunity, and it is effectively switched off upon PAMP signaling to enhance immunity and suppress growth at the same time.

DISCUSSION

We previously identified the PRE-IBH1-HBI1 tripartite HLH/bHLH cascade as an important module downstream of the BZR1-PIF-DELLA module in a central transcriptional network that mediates growth regulation by multiple hormonal and abiotic signals (Bai et al., 2012a, 2012b; Oh et al., 2012) (Figure 6). While HBI1 was shown to promote cell elongation similar to other DNA binding components of this network, its specific function in the network has remained unclear. Detailed characterization of HBI1 in this study, at both the genome-wide and molecular levels, reveals major functions of HBI1 in specifying the output of the network, feedback coordinating other components within the network, and integration of additional signals into the network. Importantly, HBI1 is activated by hormones but repressed by PAMP signals, and HBI1 both activates growth and represses immunity. Therefore, HBI1 is a key node

(B) Scatterplot of \log_2 fold change values of the genes coregulated by HBI1 and flg22. Red color indicates the HBI1 target genes. Col, Columbia.

(C) GO analyses of gene sets regulated by HBI1 and/or flg22. Numbers indicate the percentage of genes belonging to each GO category. Asterisk indicates significant difference from random genome (Fisher's exact test; $*P < 0.05$).

(D) Quantitative ChIP-PCR analysis of the HBI1 enrichment in the promoter of selected genes. The chromatin of *pHBI1:HBI1-YFP* and *35S:YFP* transgenic plants was immunoprecipitated with anti-YFP antibody, and the precipitated DNA was quantified by quantitative PCR. Enrichment of DNA was calculated as the ratio between *pHBI1:HBI1-YFP* and *35S:YFP*, normalized to that of the *PP2A* coding region. Error bars indicate standard deviation from three biological repeats. Asterisk indicates significant difference from control gene *PP2A* (*t* test; $*P < 0.05$).

(E) to **(G)** qRT-PCR analysis of flg22-regulated gene expression in wild-type (Col) and *HBI1-Ox* seedlings. Error bars indicate standard deviation from three biological repeats. Asterisk indicates significant difference from the wild type with mock treatment (*t* test; $*P < 0.05$).

(H) qRT-PCR analyses of flg22 effect on the expression of *HBI1* and *BEE2*. *PP2A* was used as the internal control. Error bars indicate standard deviation from three biological repeats. Asterisk indicates significant difference from the wild type with mock treatment (*t* test; $*P < 0.05$).

(I) Flg22 treatment reduces the HBI1-YFP protein accumulation in the *pHBI1:HBI1-YFP* but not *35S:HBI1-YFP* plants. The immunoblots were analyzed using anti-YFP antibody. The nonspecific band (asterisk) and Ponceau S staining were used to show the equal loading.

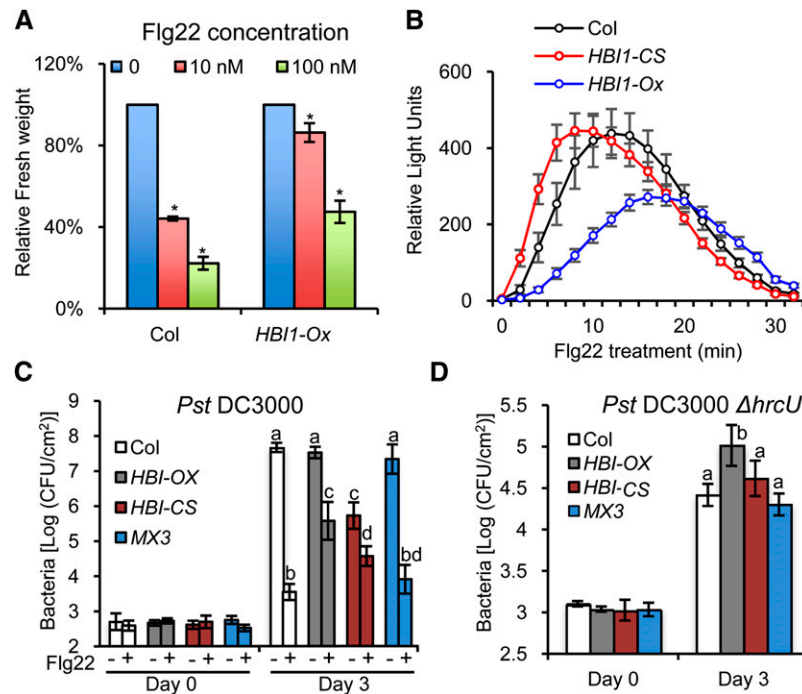


Figure 5. HBI1 Negatively Regulates PTI Signaling.

(A) *HBI1-Ox* plants show reduced sensitivity to Flg22-induced growth inhibition. Growth is represented relative to untreated plants. Error bars indicate standard deviation from three biological repeats. Asterisk indicates significant difference from mock treatment (*t* test; **P* < 0.05).

(B) Oxidative burst triggered after flg22 treatment (100 nM) in wild-type, *HBI1-CS*, and *HBI1-Ox* plants. Error bars indicate standard deviation from three biological repeats.

(C) *Pst* DC3000 growth in Columbia (Col) wild-type, *HBI-Ox*, *HBI-CS*, and *pBZR1:bzr1-1D-CFP* (*MX3*) plants pretreated with 1 μ M flg22 or water. Leaves were inoculated with 10^5 colony-forming units (CFU)/mL of bacteria. Bacterial growth was quantified at 0 and 3 d after inoculation. Data points represent mean log (colony-forming units/cm²). Error bars indicate standard deviation from 12 biological repeats. Different letters above the day 3 bars indicate statistically significant differences between the samples (one-way analysis of variance and Tukey's honestly significant difference test, *P* < 0.05).

(D) *Pst* DC3000 Δ *hrcU* growth in Columbia wild-type, *HBI-Ox*, *HBI-CS*, and *MX3* plants. Leaves were inoculated with 2×10^5 colony-forming units/mL of bacteria. Bacterial growth was quantified at 0 and 3 d after inoculation. Data points represent mean log (colony-forming units/cm²). Error bars indicate standard deviation from 12 biological repeats. Different letters above day 3 bars indicate statistically significant differences between the samples (one-way analysis of variance and Tukey's honestly significant difference test, *P* < 0.05).

for the crosstalk between growth hormones and immune signals (Figure 6).

HBI1 Promotes Cell Elongation and Feedback Regulates the Hormone Network

Our previous studies showed an essential role of the PRE-IBH1-HBI1 module in the regulation of cell elongation by several hormones, light, and temperature. HBI1 is the DNA binding bHLH factor that specifies the transcriptional output of the module (Bai et al., 2012a). Among the 1257 HBI1-regulated genes (including 177 directly regulated by HBI1 binding), HBI1 activates large numbers of genes encoding cell wall-related proteins, consistent with its role in promoting cell elongation (Bai et al., 2012b). Many of the HBI1-activated genes are also activated by PIF4, and this is likely due to overlapping function with PIF4 on shared target promoters and/or HBI1 activation of hormones. HBI1 overexpression activated genes involved in BR

biosynthesis and signal transduction and increased dephosphorylation of BZR1, suggesting a function in positive feedback regulation of upstream signaling. Such positive feedback might be important for maintaining the growth condition of young organs, as inactivation of HBI1 by elevated IBH1 expression in mature tissues (Zhang et al., 2009) would be expected to downregulate hormone synthesis and signaling. These molecular functions are consistent with HBI1's essential role in promoting cell elongation.

HBI1 also modulates the HLH/bHLH network via a feedback mechanism by transcriptionally activating IBH1 and several other HLH factors that act in parallel to IBH1 as negative regulators of growth, including PAR1, PAR2, HFR1, AIF1, AIF2, AIF3, AIF4, UPB1, and three homologs of IBH1 (Supplemental Figures 1 and 2A). Activation of these inhibitory HLH factors would inhibit not only HBI1 but also other growth-promoting bHLH factors, such as PIFs and ACEs, with which they also interact (Hornitschek et al., 2009; Bai et al., 2012a; Ikeda et al., 2012). As such, this feedback regulation would allow a change of

Taken together, our results demonstrate a central role of HBI1 in modulating a trade-off between growth and immunity. HBI1 activates growth-related genes but represses defense genes, providing opposite output for growth and defense; its activity level is posttranslationally increased by growth hormones through interaction of PREs and IBH1 but transcriptionally repressed by PAMP signaling, thereby mediating antagonistic interactions between growth and immune pathways.

Previous studies have demonstrated that the BR- and flagellin-signaling pathways share several upstream components, including the coreceptor BAK1 and the substrates BSK1 and BIK1 shared by BRI1 and FLS2 (Chinchilla et al., 2007; Kemmerling et al., 2007; Albrecht et al., 2012; Belkhadir et al., 2012; Lin et al., 2013; Shi et al., 2013). The functions of these molecular interactions in the antagonistic interaction between the two pathways remain unclear (Albrecht et al., 2012; Belkhadir et al., 2012; Lozano-Duran et al., 2013). The lack of obvious effects of BR treatment on flg22-induced BIK1 phosphorylation and of flg22 treatment on BES1 phosphorylation suggested that the sharing of upstream components does not play an important role in the crosstalk (Albrecht et al., 2012). Recently, Lozano-Duran et al. (2013) reported evidence that BZR1 mediates repression of immunity by interacting with WRKY40 and directly activating other WRKY factors that inhibit immune responses. However, we observed that *bzr1-1D* has a much weaker effect on pathogen resistance than *HBI1-Ox* or active BZR1 defective in binding to the 14-3-3 proteins, which are phosphopeptide binding proteins that prevent phospho-BZR1 from accumulating in the nucleus (Gampala et al., 2007; Lozano-Duran et al., 2013). Our latter findings may be due to lower expression of the *BZR1* mutant using the native *BZR1* promoter or a requirement of specifically abolishing the interaction with the 14-3-3 proteins. Nevertheless, both BZR1 and HBI1 directly target genes involved in immunity, and they regulate distinct sets of *WRKY* genes, suggesting that BZR1 and HBI1 contribute to inhibition of immunity through distinct transcription responses. Since HBI1 can activate BZR1 by activating the BR biosynthetic and signaling genes, and BZR1 can activate HBI1 through increasing *PRE1* expression, it is clear that HBI1 and BZR1 are parts of a positive feedback loop. Increased susceptibility caused by activation of either BZR1 or HBI1 could be partly due to indirect activation of either protein.

Unlike BZR1, which appears to be unaffected by PAMPs, HBI1 is not only activated by growth-promoting hormones but also effectively inhibited by PAMP signals. In the absence of pathogen, a high level of HBI1 activates BR synthesis and promotes growth while suppressing immunity pathways. Upon pathogen infection, PAMP-triggered repression of *HBI1* contributes to both growth inhibition and activation of immune responses. Therefore, while many molecular mechanisms may have evolved to ensure optimal balance between BR-promoted growth and PAMP-triggered immunity, our results support that HBI1 is a key node of crosstalk mediating the trade-off.

As a component of the central growth transcription network, HBI1 may mediate crosstalk between additional growth signals and PAMP signals. Previous studies have shown antagonism of PAMP signaling with auxin and GA responses. Flg22 inhibits auxin response through microRNA-mediated suppression of auxin receptors as well as a salicylic acid-dependent mechanism

to promote resistance against biotrophic pathogens (Navarro et al., 2006; Wang et al., 2007). Defense signaling also stabilizes the GA-signaling repressor DELLA proteins, which contribute to both growth inhibition and defense (Navarro et al., 2008; Yang et al., 2012). The mechanisms by which auxin and GA inhibit immunity have remained unclear. Our study suggests that auxin and GA may inhibit immunity through HBI1, as both auxin and GA activate expression of *PREs*, which activate HBI1 by sequestering IBH1 (Bai et al., 2012a). We propose that the trade-off between growth and PAMP-induced immunity in *Arabidopsis* is mainly mediated by the central growth regulation transcription network, in which HBI1 functions as a key junction between the growth and immunity pathways (Figure 6).

METHODS

Plant Materials and Growth Conditions

Arabidopsis thaliana Columbia-0 ecotype was used as wild-type control for phenotype comparison and for generating the transgenic plants. The *HBI1-Ox* and *HBI1-CS* lines have been described previously (Bai et al., 2012a). Seeds were either surface sterilized and plated on half-strength MS basal salt medium (Phyto-Technology Laboratories) or grown directly in soil.

Seedling Growth Inhibition Assay

Seedling growth inhibition was assessed as previously described (Belkhadir et al., 2012). Seedlings were grown in half-strength MS medium containing 1% Suc under constant light for 5 d, then transferred to liquid half-strength MS medium containing 1% Suc supplemented with the indicated concentration of flg22 or elf18 peptides. Seedlings were weighted 8 d after treatment.

ROS Assay

ROS assay was performed as described previously (Kunze et al., 2004). Each data point consists of at least 12 replicates.

Bacterial Growth Assays

Arabidopsis plants were grown in pots in Pro-Mix soil (Premier Horticulture) in a growth chamber (22°C, 80% RH, 125 $\mu\text{E}\cdot\text{m}^{-2}\cdot\text{s}^{-1}$ fluorescent illumination) on a 10-h-light/14-h-dark cycle. *Pst* DC3000 and *Pst* DC3000 *hrcU::Tn3gus* (*Pst* DC3000 Δ *hrcU*) mutant strain were grown on nutrient yeast glycerol agar with appropriate antibiotics (100 $\mu\text{g}/\text{mL}$ rifampicin and/or 50 $\mu\text{g}/\text{mL}$ kanamycin) at 28°C (Mudgett and Staskawicz, 1999). To monitor *Pst* DC3000 or *Pst* DC3000 Δ *hrcU* growth in plants, leaves of 4- to 5-week-old plants were hand-infiltrated with a 1 or 2 $\times 10^5$ colony-forming units/mL suspension of bacteria in 1 mM MgCl_2 using a needleless syringe. For flg22 pretreatment, the leaves were hand-infiltrated with water or 1 μM flg22 a day before the bacterial inoculation. Leaf discs per treatment per time point were collected and ground in 1 mM MgCl_2 and then spotted on nutrient yeast glycerol agar plates in triplicate to determine the bacterial titer. Each replicate includes four leaf discs and 12 biological replicates were used, and the experiment was repeated at least three times with similar results. The average bacterial titer \pm SD is reported.

Protein Gel Blot Analysis

Total protein samples were extracted from 10-d-old seedlings or 4-week-old plants using 2 \times SDS sample buffer, separated on SDS-PAGE gels,

transferred to a nitrocellulose membrane, and probed with a polyclonal anti-BZR1 antibody (custom-made, 1:1000 dilution) or anti-phosphop44/42 mitogen-activated protein kinase (Erk1/2) (Thr202/Tyr204) antibody (Cell Signaling; 1:1000 dilution).

ChIP Assay

To generate transgenic plants expressing HBI1-YFP from a native HBI1 promoter (*pHBI1:HBI1-YFP*), an *HBI1* genomic fragment including 1.3 kb upstream of the transcription start site (TSS) and all coding sequence was cloned into pENTRY/SD/D-TOPO vectors (Invitrogen) and then recombined into destination vector pEG-TW (Kim et al., 2009). The *pHBI1:HBI1-YFP* binary vector was transformed into *Agrobacterium tumefaciens* strain GV3101 and then transformed into the wild-type *Arabidopsis* (Columbia-0) plants. A line that showed wild-type phenotype but expressed detectable HBI1-YFP protein was selected and used for the ChIP assay. The *pHBI1:HBI1-YFP* and *35S:YFP* plants were grown in a greenhouse with a 16-h-light/8-h-dark cycle at 22–24°C for 4 weeks. ChIP assays were performed as described previously (Bai et al., 2012b), using an affinity-purified anti-YFP polyclonal antibody (custom-made, 10 µg for each reaction). The ChIP products were analyzed by quantitative real-time PCR (primer sequences are listed in Supplemental Table 2), and enrichment was calculated as the ratio between the transgenic samples expressing *HBI1-YFP* and the *35S:YFP* control sample. The ChIP experiments were performed with three biological replicates, from which the means and standard deviations were calculated from three biologic repeats.

ChIP-Seq Analysis

For ChIP-Seq, a library was constructed from 10 ng of ChIP DNA, pooled from 12 biological repeats to reduce sample variation, with barcodes using a NEBNext ChIP-Seq Library Prep Reagent Set for Illumina kit (New England Biolabs). Two barcode libraries were pooled together and sequenced by Illumina HiSeq2000. Total reads were mapped to the *Arabidopsis* genome (TAIR10; www.arabidopsis.org) using TopHat software (Trapnell et al., 2009). The uniquely mapped reads were analyzed using CisGenome and PRI-CAT online software with default parameters (<http://www.ab.wur.nl/pricat/>) (Ji et al., 2008; Muñoz et al., 2011). The data of the *35S:YFP* sample were used as a negative control, and the HBI1 binding peaks were defined using fold change >1.5, false discovery rate-adjusted P value < 0.05. Two nearest neighbor genes flanking each binding site and genes that contain binding site within the transcribed region were defined as putative HBI1 binding target genes.

To discover the in vivo HBI1 binding motifs, DNA sequences of the binding peaks were analyzed by MEME-ChIP (Machanick and Bailey, 2011). The motifs identified by MEME-ChIP were further analyzed by comparing the frequencies of the motifs in the binding peaks to those in the *Arabidopsis* total genome (TAIR9; www.arabidopsis.org).

To determine the genomic distribution of HBI1 binding peaks relative to gene structure, we divided the genome into three regions: 5 kb upstream of the TSS to TSS, the TSS to the 3' end of the gene, and the 3' end of the gene to 1 kb downstream of the gene. We then calculated the frequency of binding peaks in these three regions. If a peak was located within 5 kb upstream of one gene and 1 kb downstream of another gene, the peak was counted in both regions. Peaks outside these regions were not included and peaks existing within 5 kb upstream of two different genes were counted twice.

qRT-PCR Analysis

Total RNA was extracted from *Arabidopsis* seedlings using the Spectrum Plant Total RNA kit (Sigma-Aldrich). The first-strand cDNA was synthesized

using RevertAid reverse transcriptase (Fermentas) and used as RT-PCR templates. Quantitative PCR analyses were performed on a plate-based LightCycler 480 (Roche) using a SYBR Green reagent (Bio-Rad) with gene-specific primers (Supplemental Table 2). The conditions for PCR amplification were as follows: 98°C for 10 min; 45 cycles of 98°C for 30 s; 65°C for 45 s and 72°C for 30 s; one cycle of 72°C for 10 min. The relative expression was calculated as ratio between the transgenic plant and the wild type and then normalized by the *PP2A* (AT1G13320) gene, which is a constitutively expressed reference gene (Czechowski et al., 2005). The means and standard deviations were calculated from three biological repeats.

RNA-Seq Analysis

Plants were grown on half-strength MS medium for 5 d under constant light. Total RNA was extracted from two biological repeat samples with the Spectrum Plant Total RNA Kit (Sigma-Aldrich), and mRNA sequencing libraries were constructed with barcodes using the TrueSeq RNA Sample Preparation Kit (Illumina). Four barcoded libraries were pooled together and sequenced by Illumina HiSeq2000. Total reads were mapped to the *Arabidopsis* genome (TAIR10; www.arabidopsis.org) using the TopHat software (Trapnell et al., 2009). Read counts for every gene were generated using HTSeq with union mode. Differential expressed genes between samples were defined by DESeq using two separate models (Anders and Huber, 2010), based on fold change >1.5 and false discovery rate-adjusted P value < 0.05. Gene Ontology analysis was assisted by the *VirtualPlant* package (Katari et al., 2010), and the functional categories were determined using the annotation of the *Arabidopsis* genome (TAIR10; www.arabidopsis.org).

Accession Numbers

Sequence data for ChIP-Seq and RNA-Seq can be found in the Gene Expression Omnibus database under accession numbers GSE53099 and GSE53078.

Supplemental Data

The following materials are available in the online version of this article.

Supplemental Figure 1. Representative HBI1 Binding and Regulated Genes with Known Functions in Various Developmental and Cellular Processes.

Supplemental Figure 2. Growth-Promoting and Growth-Inhibiting HLH Factors Are Directly Repressed and Induced by HBI1, Respectively.

Supplemental Figure 3. HBI1 and PIF Have Overlapping and Distinct Functions.

Supplemental Figure 4. HBI1 Negatively Regulates elf18- and flg22-Mediated PTI Responses.

Supplemental Figure 5. Activation of HBI1 Results in the Suppression of PTI Marker Gene Expression but Not MAPK Activation.

Supplemental Figure 6. Quantitative RT-PCR Analyses of flg22 Effect on the Expression of HBI1 Homolog Genes.

Supplemental Table 1. Quantitative RT-PCR Validation of the RNA-Seq Data.

Supplemental Table 2. Oligonucleotide Sequences Used in This Study.

Supplemental Data Set 1. ChIP-Seq Analysis of HBI1 Binding Sites.

Supplemental Data Set 2. RNA-Seq Analysis of Genes Affected in *HBI1-Ox* Plants.

ACKNOWLEDGMENTS

We thank the Stanford Center for Genomics and Personalized Medicine led by Michael Snyder and Arend Sidow for the sequencing service and Ziming Weng for carrying out the sequencing. This study was supported by grants from the National Institutes of Health (R01GM066258 to Z.-Y.W. and 2R01GM068886-06A1 to M.B.M.), a “Qilu Scholarship” from Shandong University of China (11200083963009 to M.-Y.B.), and the National Research Foundation of Korea Grant funded by the Korean Government (NRF-2011-220-C00059 to S.-K.K.). We declare no competing financial interests.

AUTHOR CONTRIBUTIONS

M.-Y.B. and Z.-Y.W. designed the experiments. M.-Y.B. performed ChIP-Seq, RNA-Seq, and together with E.O. analyzed sequencing data. M.F. together with T.W. and L.C. performed ROS burst assay, RT-qPCR, ChIP-qPCR, and statistical analysis of plant growth. J.-G.K. performed pathogen growth assays. J.-G.K. and M.B.M. helped with data interpretation and article editing. M.F. performed all other experiments. M.-Y.B. and Z.-Y.W. wrote the article.

Received November 24, 2013; revised January 18, 2014; accepted January 24, 2014; published February 18, 2014.

REFERENCES

- Albrecht, C., Boutrot, F., Segonzac, C., Schwessinger, B., Gimenez-Ibanez, S., Chinchilla, D., Rathjen, J.P., de Vries, S.C., and Zipfel, C. (2012). Brassinosteroids inhibit pathogen-associated molecular pattern-triggered immune signaling independent of the receptor kinase BAK1. *Proc. Natl. Acad. Sci. USA* **109**: 303–308.
- Anders, S., and Huber, W. (2010). Differential expression analysis for sequence count data. *Genome Biol.* **11**: R106.
- Bai, M.Y., Fan, M., Oh, E., and Wang, Z.Y. (2012a). A triple helix-loop-helix/basic helix-loop-helix cascade controls cell elongation downstream of multiple hormonal and environmental signaling pathways in *Arabidopsis*. *Plant Cell* **24**: 4917–4929.
- Bai, M.Y., Shang, J.X., Oh, E., Fan, M., Bai, Y., Zentella, R., Sun, T.P., and Wang, Z.Y. (2012b). Brassinosteroid, gibberellin and phytochrome impinge on a common transcription module in *Arabidopsis*. *Nat. Cell Biol.* **14**: 810–817.
- Belkhadir, Y., Jaillais, Y., Epple, P., Balsemão-Pires, E., Dangl, J.L., and Chory, J. (2012). Brassinosteroids modulate the efficiency of plant immune responses to microbe-associated molecular patterns. *Proc. Natl. Acad. Sci. USA* **109**: 297–302.
- Bethke, G., Pecher, P., Eschen-Lippold, L., Tsuda, K., Katagiri, F., Glazebrook, J., Scheel, D., and Lee, J. (2012). Activation of the *Arabidopsis thaliana* mitogen-activated protein kinase MPK11 by the flagellin-derived elicitor peptide, flg22. *Mol. Plant Microbe Interact.* **25**: 471–480.
- Cheng, Y., Zhou, Y., Yang, Y., Chi, Y.J., Zhou, J., Chen, J.Y., Wang, F., Fan, B., Shi, K., Zhou, Y.H., Yu, J.Q., and Chen, Z. (2012). Structural and functional analysis of VQ motif-containing proteins in *Arabidopsis* as interacting proteins of WRKY transcription factors. *Plant Physiol.* **159**: 810–825.
- Chiasson, D., Ekengren, S.K., Martin, G.B., Dobney, S.L., and Snedden, W.A. (2005). Calmodulin-like proteins from *Arabidopsis* and tomato are involved in host defense against *Pseudomonas syringae* pv. tomato. *Plant Mol. Biol.* **58**: 887–897.
- Chinchilla, D., Zipfel, C., Robatzek, S., Kemmerling, B., Nürnberger, T., Jones, J.D., Felix, G., and Boller, T. (2007). A flagellin-induced complex of the receptor FLS2 and BAK1 initiates plant defence. *Nature* **448**: 497–500.
- Czechowski, T., Stitt, M., Altmann, T., Udvardi, M.K., and Scheible, W.R. (2005). Genome-wide identification and testing of superior reference genes for transcript normalization in *Arabidopsis*. *Plant Physiol.* **139**: 5–17.
- de Lucas, M., Davière, J.M., Rodríguez-Falcón, M., Pontin, M., Iglesias-Pedraz, J.M., Lorrain, S., Fankhauser, C., Blázquez, M.A., Titarenko, E., and Prat, S. (2008). A molecular framework for light and gibberellin control of cell elongation. *Nature* **451**: 480–484.
- Denoux, C., Galletti, R., Mammarella, N., Gopalan, S., Werck, D., De Lorenzo, G., Ferrari, S., Ausubel, F.M., and Dewdney, J. (2008). Activation of defense response pathways by OGs and Flg22 elicitors in *Arabidopsis* seedlings. *Mol. Plant* **1**: 423–445.
- Depuydt, S., and Hardtke, C.S. (2011). Hormone signalling crosstalk in plant growth regulation. *Curr. Biol.* **21**: R365–R373.
- Feng, S., et al. (2008). Coordinated regulation of *Arabidopsis thaliana* development by light and gibberellins. *Nature* **451**: 475–479.
- Gallego-Bartolomé, J., Minguet, E.G., Grau-Enguix, F., Abbas, M., Locascio, A., Thomas, S.G., Alabadí, D., and Blázquez, M.A. (2012). Molecular mechanism for the interaction between gibberellin and brassinosteroid signaling pathways in *Arabidopsis*. *Proc. Natl. Acad. Sci. USA* **109**: 13446–13451.
- Gampala, S.S., et al. (2007). An essential role for 14-3-3 proteins in brassinosteroid signal transduction in *Arabidopsis*. *Dev. Cell* **13**: 177–189.
- Göhre, V., Jones, A.M., Sklenář, J., Robatzek, S., and Weber, A.P. (2012). Molecular crosstalk between PAMP-triggered immunity and photosynthesis. *Mol. Plant Microbe Interact.* **25**: 1083–1092.
- Hao, Y., Oh, E., Choi, G., Liang, Z., and Wang, Z.Y. (2012). Interactions between HLH and bHLH factors modulate light-regulated plant development. *Mol. Plant* **5**: 688–697.
- Hiruma, K., Fukunaga, S., Bednarek, P., Pislewska-Bednarek, M., Watanabe, S., Narusaka, Y., Shirasu, K., and Takano, Y. (2013). Glutathione and tryptophan metabolism are required for *Arabidopsis* immunity during the hypersensitive response to hemibiotrophs. *Proc. Natl. Acad. Sci. USA* **110**: 9589–9594.
- Hornitschek, P., Kohnen, M.V., Lorrain, S., Rougemont, J., Ljung, K., López-Vidriero, I., Franco-Zorrilla, J.M., Solano, R., Trevisan, M., Pradervand, S., Xenarios, I., and Fankhauser, C. (2012). Phytochrome interacting factors 4 and 5 control seedling growth in changing light conditions by directly controlling auxin signaling. *Plant J.* **71**: 699–711.
- Hornitschek, P., Lorrain, S., Zoete, V., Michielin, O., and Fankhauser, C. (2009). Inhibition of the shade avoidance response by formation of non-DNA binding bHLH heterodimers. *EMBO J.* **28**: 3893–3902.
- Hyun, Y., and Lee, I. (2006). KIDARI, encoding a non-DNA binding bHLH protein, represses light signal transduction in *Arabidopsis thaliana*. *Plant Mol. Biol.* **61**: 283–296.
- Ikeda, M., Fujiwara, S., Mitsuda, N., and Ohme-Takagi, M. (2012). A triantagonistic basic helix-loop-helix system regulates cell elongation in *Arabidopsis*. *Plant Cell* **24**: 4483–4497.
- Ji, H., Jiang, H., Ma, W., Johnson, D.S., Myers, R.M., and Wong, W.H. (2008). An integrated software system for analyzing ChIP-chip and ChIP-seq data. *Nat. Biotechnol.* **26**: 1293–1300.
- Katari, M.S., Nowicki, S.D., Aceituno, F.F., Nero, D., Kelfer, J., Thompson, L.P., Cabello, J.M., Davidson, R.S., Goldberg, A.P., Shasha, D.E., Coruzzi, G.M., and Gutiérrez, R.A. (2010). VirtualPlant: A software platform to support systems biology research. *Plant Physiol.* **152**: 500–515.

- Kemmerling, B., et al.** (2007). The BRI1-associated kinase 1, BAK1, has a brassinolide-independent role in plant cell-death control. *Curr. Biol.* **17**: 1116–1122.
- Kim, T.W., Guan, S., Burlingame, A.L., and Wang, Z.Y.** (2011). The CDG1 kinase mediates brassinosteroid signal transduction from BRI1 receptor kinase to BSU1 phosphatase and GSK3-like kinase BIN2. *Mol. Cell* **43**: 561–571.
- Kim, T.W., Guan, S., Sun, Y., Deng, Z., Tang, W., Shang, J.X., Sun, Y., Burlingame, A.L., and Wang, Z.Y.** (2009). Brassinosteroid signal transduction from cell-surface receptor kinases to nuclear transcription factors. *Nat. Cell Biol.* **11**: 1254–1260.
- Kim, T.W., and Wang, Z.Y.** (2010). Brassinosteroid signal transduction from receptor kinases to transcription factors. *Annu. Rev. Plant Biol.* **61**: 681–704.
- Ko, C.B., Woo, Y.M., Lee, D.J., Lee, M.C., and Kim, C.S.** (2007). Enhanced tolerance to heat stress in transgenic plants expressing the GASA4 gene. *Plant Physiol. Biochem.* **45**: 722–728.
- Kunze, G., Zipfel, C., Robatzek, S., Niehaus, K., Boller, T., and Felix, G.** (2004). The N terminus of bacterial elongation factor Tu elicits innate immunity in *Arabidopsis* plants. *Plant Cell* **16**: 3496–3507.
- Lai, Z., Li, Y., Wang, F., Cheng, Y., Fan, B., Yu, J.Q., and Chen, Z.** (2011). *Arabidopsis* sigma factor binding proteins are activators of the WRKY33 transcription factor in plant defense. *Plant Cell* **23**: 3824–3841.
- Li, J., Wen, J., Lease, K.A., Doke, J.T., Tax, F.E., and Walker, J.C.** (2002). BAK1, an *Arabidopsis* LRR receptor-like protein kinase, interacts with BRI1 and modulates brassinosteroid signaling. *Cell* **110**: 213–222.
- Li, Q.-F., Wang, C., Jiang, L., Li, S., Sun, S.S., and He, J.X.** (2012). An interaction between BZR1 and DELLAs mediates direct signaling crosstalk between brassinosteroids and gibberellins in *Arabidopsis*. *Sci. Signal.* **5**: ra72.
- Lin, W., Lu, D., Gao, X., Jiang, S., Ma, X., Wang, Z., Mengiste, T., He, P., and Shan, L.** (2013). Inverse modulation of plant immune and brassinosteroid signaling pathways by the receptor-like cytoplasmic kinase BIK1. *Proc. Natl. Acad. Sci. USA* **110**: 12114–12119.
- Lozano-Durán, R., Macho, A.P., Boutrot, F., Segonzac, C., Somssich, I.E., and Zipfel, C.** (2013). The transcriptional regulator BZR1 mediates trade-off between plant innate immunity and growth. *Elife* **2**: e00983.
- Lu, D., Wu, S., Gao, X., Zhang, Y., Shan, L., and He, P.** (2010). A receptor-like cytoplasmic kinase, BIK1, associates with a flagellin receptor complex to initiate plant innate immunity. *Proc. Natl. Acad. Sci. USA* **107**: 496–501.
- Machanick, P., and Bailey, T.L.** (2011). MEME-ChIP: Motif analysis of large DNA datasets. *Bioinformatics* **27**: 1696–1697.
- Michael, T.P., Breton, G., Hazen, S.P., Priest, H., Mockler, T.C., Kay, S.A., and Chory, J.** (2008). A morning-specific phytohormone gene expression program underlying rhythmic plant growth. *PLoS Biol.* **6**: e225.
- Møldrup, M.E., Salomonsen, B., Geu-Flores, F., Olsen, C.E., and Halkier, B.A.** (2013). De novo genetic engineering of the camalexin biosynthetic pathway. *J. Biotechnol.* **167**: 296–301.
- Mudgett, M.B., and Staskawicz, B.J.** (1999). Characterization of the *Pseudomonas syringae* pv. tomato AvrRpt2 protein: demonstration of secretion and processing during bacterial pathogenesis. *Mol. Microbiol.* **32**: 927–941.
- Muñoz, J.M., Hoogstraal, M., van Ham, R.C.H.J., and van Dijk, A.D.J.** (2011). PRI-CAT: A web-tool for the analysis, storage and visualization of plant ChIP-seq experiments. *Nucleic Acids Res.* **39**: W524–7.
- Nahirňak, V., Almasia, N.I., Hopp, H.E., and Vazquez-Rovere, C.** (2012). Snakin/GASA proteins: Involvement in hormone crosstalk and redox homeostasis. *Plant Signal. Behav.* **7**: 1004–1008.
- Nam, K.H., and Li, J.** (2002). BRI1/BAK1, a receptor kinase pair mediating brassinosteroid signaling. *Cell* **110**: 203–212.
- Navarro, L., Bari, R., Achard, P., Lisón, P., Nemri, A., Harberd, N.P., and Jones, J.D.** (2008). DELLAs control plant immune responses by modulating the balance of jasmonic acid and salicylic acid signaling. *Curr. Biol.* **18**: 650–655.
- Navarro, L., Dunoyer, P., Jay, F., Arnold, B., Dharmasiri, N., Estelle, M., Voinnet, O., and Jones, J.D.G.** (2006). A plant miRNA contributes to antibacterial resistance by repressing auxin signaling. *Science* **312**: 436–439.
- Oh, E., Kang, H., Yamaguchi, S., Park, J., Lee, D., Kamiya, Y., and Choi, G.** (2009). Genome-wide analysis of genes targeted by PHYTOCHROME INTERACTING FACTOR 3-LIKE5 during seed germination in *Arabidopsis*. *Plant Cell* **21**: 403–419.
- Oh, E., Zhu, J.Y., and Wang, Z.Y.** (2012). Interaction between BZR1 and PIF4 integrates brassinosteroid and environmental responses. *Nat. Cell Biol.* **14**: 802–809.
- Robert-Seilaniantz, A., Grant, M., and Jones, J.D.** (2011). Hormone crosstalk in plant disease and defense: More than just jasmonate-salicylate antagonism. *Annu. Rev. Phytopathol.* **49**: 317–343.
- Roxrud, I., Lid, S.E., Fletcher, J.C., Schmidt, E.D., and Opsahl-Sorteberg, H.G.** (2007). GASA4, one of the 14-member *Arabidopsis* GASA family of small polypeptides, regulates flowering and seed development. *Plant Cell Physiol.* **48**: 471–483.
- Rubinovich, L., and Weiss, D.** (2010). The *Arabidopsis* cysteine-rich protein GASA4 promotes GA responses and exhibits redox activity in bacteria and in planta. *Plant J.* **64**: 1018–1027.
- Santiago, J., Henzler, C., and Hothorn, M.** (2013). Molecular mechanism for plant steroid receptor activation by somatic embryogenesis co-receptor kinases. *Science* **341**: 889–892.
- Shi, H., Shen, Q., Qi, Y., Yan, H., Nie, H., Chen, Y., Zhao, T., Katagiri, F., and Tang, D.** (2013). BR-SIGNALING KINASE1 physically associates with FLAGELLIN SENSING2 and regulates plant innate immunity in *Arabidopsis*. *Plant Cell* **25**: 1143–1157.
- Sun, S., Wang, H., Yu, H., Zhong, C., Zhang, X., Peng, J., and Wang, X.** (2013). GASA14 regulates leaf expansion and abiotic stress resistance by modulating reactive oxygen species accumulation. *J. Exp. Bot.* **64**: 1637–1647.
- Sun, T.P.** (2011). The molecular mechanism and evolution of the GA-GID1-DELLA signaling module in plants. *Curr. Biol.* **21**: R338–R345.
- Sun, Y., et al.** (2010). Integration of brassinosteroid signal transduction with the transcription network for plant growth regulation in *Arabidopsis*. *Dev. Cell* **19**: 765–777.
- Tang, W., Kim, T.W., Osés-Prieto, J.A., Sun, Y., Deng, Z., Zhu, S., Wang, R., Burlingame, A.L., and Wang, Z.Y.** (2008). BSKs mediate signal transduction from the receptor kinase BRI1 in *Arabidopsis*. *Science* **321**: 557–560.
- Tang, W., et al.** (2011). PP2A activates brassinosteroid-responsive gene expression and plant growth by dephosphorylating BZR1. *Nat. Cell Biol.* **13**: 124–131.
- Tintor, N., Ross, A., Kanehara, K., Yamada, K., Fan, L., Kemmerling, B., Nürnberger, T., Tsuda, K., and Saijo, Y.** (2013). Layered pattern receptor signaling via ethylene and endogenous elicitor peptides during *Arabidopsis* immunity to bacterial infection. *Proc. Natl. Acad. Sci. USA* **110**: 6211–6216.
- Trapnell, C., Pachter, L., and Salzberg, S.L.** (2009). TopHat: Discovering splice junctions with RNA-Seq. *Bioinformatics* **25**: 1105–1111.
- Trujillo, M., Ichimura, K., Casais, C., and Shirasu, K.** (2008). Negative regulation of PAMP-triggered immunity by an E3 ubiquitin ligase triplet in *Arabidopsis*. *Curr. Biol.* **18**: 1396–1401.
- Wang, D., Pajerowska-Mukhtar, K., Culler, A.H., and Dong, X.** (2007). Salicylic acid inhibits pathogen growth in plants through repression of the auxin signaling pathway. *Curr. Biol.* **17**: 1784–1790.

- Wang, X., Kota, U., He, K., Blackburn, K., Li, J., Goshe, M.B., Huber, S.C., and Clouse, S.D.** (2008). Sequential transphosphorylation of the BRI1/BAK1 receptor kinase complex impacts early events in brassinosteroid signaling. *Dev. Cell* **15**: 220–235.
- Wang, Z.Y., Bai, M.Y., Oh, E., and Zhu, J.Y.** (2012). Brassinosteroid signaling network and regulation of photomorphogenesis. *Annu. Rev. Genet.* **46**: 701–724.
- Xie, Y.D., Li, W., Guo, D., Dong, J., Zhang, Q., Fu, Y., Ren, D., Peng, M., and Xia, Y.** (2010). The *Arabidopsis* gene SIGMA FACTOR-BINDING PROTEIN 1 plays a role in the salicylate- and jasmonate-mediated defence responses. *Plant Cell Environ.* **33**: 828–839.
- Yang, D.L., et al.** (2012). Plant hormone jasmonate prioritizes defense over growth by interfering with gibberellin signaling cascade. *Proc. Natl. Acad. Sci. USA* **109**: E1192–E1200.
- Yu, X., Li, L., Zola, J., Aluru, M., Ye, H., Foudree, A., Guo, H., Anderson, S., Aluru, S., Liu, P., Rodermeil, S., and Yin, Y.** (2011). A brassinosteroid transcriptional network revealed by genome-wide identification of BES1 target genes in *Arabidopsis thaliana*. *Plant J.* **65**: 634–646.
- Zhang, L.Y., et al.** (2009). Antagonistic HLH/bHLH transcription factors mediate brassinosteroid regulation of cell elongation and plant development in rice and *Arabidopsis*. *Plant Cell* **21**: 3767–3780.
- Zhang, Y., Mayba, O., Pfeiffer, A., Shi, H., Tepperman, J.M., Speed, T.P., and Quail, P.H.** (2013). A quartet of PIF bHLH factors provides a transcriptionally centered signaling hub that regulates seedling morphogenesis through differential expression-patterning of shared target genes in *Arabidopsis*. *PLoS Genet.* **9**: e1003244.